arXiv:1405.0260v2 [math.NA] 5 Nov 2014

A PARALLEL ORBITAL-UPDATING APPROACH FOR ELECTRONIC STRUCTURE CALCULATIONS *

XIAOYING DAI†, XINGAO GONG‡, AIHUI ZHOU† , AND JINWEI ZHU†

Abstract. In this paper, we propose an orbital iteration based parallel approach for electronic structure calculations. This approach is based on our understanding of the single-particle equations of independent particles that move in an effective potential. With this new approach, the solution of the single-particle equation is reduced to some solutions of independent linear algebraic systems and a small scale algebraic problem. It is demonstrated by our numerical experiments that this new approach is quite efficient for full-potential calculations for a class of molecular systems.

Key words. eigenvalue, eigenspace, electronic structure, finite element, full-potential calculation, parallel orbital-updating

AMS subject classification. 35Q55, 65N25, 65N30, 65N50, 81Q05

1. Introduction.

The many-body Schrödinger equation for electronic structure is usually intractable. In applications, simplified and equivalent models that are tractable are then desired and proposed. Among them there are single-particle approximations, such as Hartree-Fock type equation and Kohn-Sham equations[18, 19, 21, 23, 25].

Within the framework of the single-particle approximation, the original intractable many-body Schrödinger equation is reduced to a set of tractable single-particle equations of independent particles that move in an effective potential, while the effective potential includes an external potential defined by the nuclei or ions and the effects of the electron-electron interactions. It is a quite good description when effects of exchange and correlation are not crucial for describing the phenomena required. The Kohn-Sham equation, for instance, is the group of single-particle equations for non-interacting quasi-particles, whose density is the same as the exact density of real electrons. The various physical quantities can be expressed in terms of the single-particle orbitals. With these single-particle approximations, we observe that the orbitals may be computed individually or in parallel.

The main philosophy behind this paper is that a fundamental algorithm must be built on simple rules. Indeed, supercomputers would otherwise be unable to cope with it efficiently. We understand that the rules of fundamental physical theories on motions are very simple while the complexity of a system results from its specificity of initial condition, like Newtonian laws. In our approach, we try to use this kind of idea for designing discretization schemes. We note that an iteration process may be viewed as (a discretized version of) some motion. Motivated by such a consideration and observation, in this paper, we will propose a new parallel approach for electronic structure calculations based on finite element discretizations and some simple iterations. The approach may be viewed as a single-particle orbital updating algorithm.

*This work was partially supported by the Funds for Creative Research Groups of China under grant 11321061, the National Basic Research Program of China under grant 2011CB309703, the National Science Foundation of China under grants 11101416 and 91330202, the National 863 Project of China under grant 2012AA01A309, and the National Center for Mathematics and Interdisciplinary Sciences of Chinese Academy of Sciences.

†LSEC, Institute of Computational Mathematics and Scientific/Engineering Computing, Academy of Mathematics and Systems Science, Chinese Academy of Sciences, Beijing 100190, China (daixy, azhou, jwzhu@lsec.cc.ac.cn).

‡ Department of Physics, Fudan University, Shanghai 200433, China (xggong@fudan.edu.cn).

It is shown by our investigation that a simple iteration with some observational data would be efficient for a special situation and supercomputers. One prototype algorithm for electronic structure calculations based on finite element discretizations is stated as follows (see Section 3.2):

ALGORITHM 1.1.

1. *Given initial data* $(\lambda_i^{(0)}, u_i^{(0)}) \in \mathbb{R} \times H_0^1(\Omega)$ *with* $(u_i^{(0)}, u_j^{(0)})_\Omega = \delta_{ij}, (i, j = 1, 2, \cdots, N)$, *define* $\mathcal{T}_0$ *and* V_0, *and let* $n = 0$
2. *Construct* $\mathcal{T}_{n+1}$ *and* V_{n+1} *based on an adaptive procedure to* $(\lambda_i^{(n)}, u_i^{(n)})$.
3. *For* $i = 1, 2, \cdots, N$, *find* $u_i^{(n+1/2)} \in V_{n+1}$ *satisfying*

$$a(U^{(n)}; u_i^{(n+1/2)}, v) = \lambda_i^{(n)}(u_i^{(n)}, v) \ \forall v \in V_{n+1}$$

   in parallel.
4. *Project to eigenspace: find* $(\lambda^{(n+1)}, u^{(n+1)}) \in \mathbb{R} \times \tilde{V}_{n+1}$ *satisfying* $\|u^{(n+1)}\|_{0,\Omega} = 1$ *and*

$$a(U^{(n+1/2)}; u^{(n+1)}, v) = \lambda^{(n+1)}(u^{(n+1)}, v) \quad \forall v \in \tilde{V}_{n+1}$$

   to obtain eigenpairs $(\lambda_i^{(n+1)}, u_i^{(n+1)})(i = 1, 2, \cdots, N)$.
5. *Let* $n = n + 1$ *and go to Step 2.*

Here $\tilde{V}_{n+1} = \text{span}\{u_1^{(n+1/2)}, u_2^{(n+1/2)}, \cdots, u_N^{(n+1/2)}\}$, $U^{(n)} = (u_1^{(n)}, u_2^{(n)}, \cdots, u_N^{(n)})$, $U^{(n+1/2)} = (u_1^{(n+1/2)}, u_2^{(n+1/2)}, \cdots, u_N^{(n+1/2)})$, *and* $a(\cdot; \cdot, \cdot)$ *is the nonlinear variational form associated the Kohn-Sham equation defined in Section 2.2.*

We understand that modern computational science does not have an algorithm setting up initial conditions, it can only determine initial conditions through physical observation and data. In Step 1 of Algorithm 1.1, we may choose

- Gaussian-type orbital or Slater-type orbital based guesses, which are applicable to full-potential calculations,
- local plane-wave discretization based guesses, which are applicable to pseudo-potential settings,
- local finite element/volume discretization based guesses, which are applicable to either full-potential calculations or pseudo-potential settings.

Step 2 is used to deal with the singularity of Coulomb potentials or the highly oscillating behaviors of eigenfunctions. Step 3 is to solve some source problems while Step 4 is an eigenvalue problem of small scale.

Note that Kohn-Sham equation is a nonlinear eigenvalue problem. To handle the nonlinearity, the so called self-consistent field (SCF) (see, e.g., [20, 24]) iteration approach is usually applied. After some discretization, the central computation of such kind of nonlinear eigenvalue problems is the repeat computation of the following algebraic eigenvalue problem

$$Au = \lambda Bu,$$

where A is the stiff matrix, B is the mass matrix. For the above algebraic eigenvalue problem, we need to solve the first N eigenvalues and the corresponding eigenfunctions or eigenspaces. If A and B are sparse, then the optimal computational complexity is $\mathcal{O}(N^2 N_g)$, while if A or B is dense, then the optimal computational complexity is $\mathcal{O}(N N_g^2)$. Here N_g is the dimension of the matrix. Using a finite element, finite difference or finite volume method to discretize Kohn-Sham equation is the former case, while using plane wave functions as the bases or use Gaussian type bases belong

to the latter case. Usually, one need to solve tens of such algebraic eigenvalue problem, and either $N_g \gg N$ or a practically complete basis set is difficult to obtain [4, 5, 6, 22, 28, 29]. So, the cost will be the lowest when N_g becomes N.

With this new algorithm, we see that the solution of the original tens of large scale eigenvalue problems will be reduced to the solution of some independent source problems and some eigenvalue problem of small scales. Consequently, the optimal computational complexity becomes $\mathcal{O}(N_g + N^3)$, which is much lower than either $\mathcal{O}(N^2 N_g)$ or $\mathcal{O}(N N_g^2)$. Besides, since the N source problems in Step 3 are independent each other, they can be calculated in parallel intrinsically. This indicates that our algorithm can use more processors and hence possesses a supercomputing potential.

The rest of this paper is organized as follows. In Section 2, we provide some preliminaries for Kohn-Sham DFT problem setting. We then propose our new parallel orbital-updating approach for electronic structure calculations in Section 3. In Section 4, we present some numerical experiments that show the efficiency of our new algorithm. Finally, we give some concluding remarks and an appendix.

2. Preliminaries. Let $\Omega \subset \mathbb{R}^3$ be a polyhedral domain. We shall use the standard notation for Sobolev spaces $H^s(\Omega)(1 \le s < \infty)$ and their associated norms and seminorms, see, e.g., [1]. We denote $H_0^1(\Omega) = \{v \in H^1(\Omega) : v\,|_{\partial\Omega} = 0\}$, where $v\,|_{\partial\Omega} = 0$ is understood in the sense of trace and $(\cdot,\cdot)$ is the standard L^2 inner product.

Let $\{\mathcal{T}_h\}$ be a shape regular family of nested conforming meshes over Ω with size h that is small enough: there exists a constant γ^* such that

$$\frac{h_\tau}{\rho_\tau} \le \gamma^* \quad \forall\, \tau \in \mathcal{T}_h, \tag{2.1}$$

where h_τ is the diameter of τ for each $\tau \in \mathcal{T}_h$, ρ_τ is the diameter of the biggest ball contained in τ, and $h = \max\{h_\tau : \tau \in \mathcal{T}_h\}$. Let $\mathcal{E}_h$ denote the set of interior faces (edges or sides) of $\mathcal{T}_h$.

Let $S^{h,k}(\Omega)$ be a subspace of continuous functions on Ω such that

$$S^{h,k}(\Omega) = \{v \in C(\bar{\Omega}) :\ v|_\tau \in P_\tau^k \quad \forall\, \tau \in \mathcal{T}_h\},$$

where P_τ^k is the space of polynomials of degree no greater than k over τ. $S^{h,k}(\Omega)$ are usually called finite element spaces. Let $S_0^{h,k}(\Omega) = S^{h,k}(\Omega) \cap H_0^1(\Omega)$. We shall denote $S_0^{h,k}(\Omega)$ by $S_0^h(\Omega)$ for simplification of notation afterwards.

2.1. Adaptive finite element approximation. To handle the Coulomb potential or the highly oscillating behaviors of eigenfunctions efficiently, we apply an adaptive finite element approach to discretize the associated source problems. An adaptive finite element algorithm usually consists of the following loop [7, 8, 10, 12]:

$$\textbf{Solve} \ \rightarrow\ \textbf{Estimate} \ \rightarrow\ \textbf{Mark} \ \rightarrow\ \textbf{Refine}.$$

We shall replace the subscript h (or h_k) by an iteration counter k whenever convenient afterwards.

Solve. Get the piecewise polynomial finite element approximation with respect to a given mesh $\mathcal{T}_k$.

Estimate. Given a mesh $\mathcal{T}_k$ and the corresponding output from the "Solve" step, "Estimate" presents the a posteriori error estimators $\{\eta_k(\cdot,\tau)\}_{\tau\in\mathcal{T}_k}$.

Mark. Based on the a posteriori error indicators $\{\eta_k(\cdot,\tau)\}_{\tau\in\mathcal{T}_k}$, "Mark" provides a strategy to choose a subset $\mathcal{M}_k$ of elements of $\mathcal{T}_k$ for refining.

Refine. Associated with the mesh $\mathcal{T}_k$ and the set of marked elements $\mathcal{M}_k$, "Refine" produces a new mesh $\mathcal{T}_{k+1}$ by refining all elements in $\mathcal{M}_k$ at least one time.

One of the most widely used marking strategy to enforce error reduction is the following so-called Dörfler strategy [14].

Dörfler Strategy. Given a marking parameter $0 < \theta < 1$:

1. Choose a subset $\mathcal{M}_k \subset \mathcal{T}_k$ such that

$$\sum_{\tau \in \mathcal{M}_k} \eta_k^2(\cdot, \tau) \geq \theta \sum_{\tau \in \mathcal{T}_k} \eta_k^2(\cdot, \tau). \tag{2.2}$$

2. Mark all the elements in $\mathcal{M}_k$.

The "Maximum Strategy" is another wildly used marking strategy.

Maximum Strategy. Given a marking parameter $0 < \theta < 1$:

1. Choose a subset $\mathcal{M}_k \subset \mathcal{T}_k$ such that

$$\eta_k(\cdot, \tau) \geq \theta \max_{\tau \in \mathcal{T}_k} \eta_k(\cdot, \tau). \tag{2.3}$$

2. Mark all the elements in $\mathcal{M}_k$.

In our computation, we apply the shape-regular bisection for the refinement. We refer to [8, 10] for more details for the adaptive finite element computations for Kohn-Sham DFT.

2.2. Kohn-Sham equation. The Kohn-Sham equation of a molecular system consisting of M nuclei of charges $\{Z_1, \cdots, Z_M\}$ located at positions $\{\mathbf{R}_1, \cdots, \mathbf{R}_M\}$ and N_e electrons in the non-relativistic and spin-unpolarized setting is the following nonlinear eigenvalue problem

$$\begin{cases} \left(-\frac{1}{2}\Delta + V_{\text{ext}} + V_H(\rho) + V_{\text{xc}}(\rho)\right) u_i &= \lambda_i u_i \quad \text{in } \mathbb{R}^3, \\ \displaystyle\int_{\mathbb{R}^3} u_i u_j &= \delta_{ij}, \quad i, j = 1, 2, \cdots, N, \end{cases} \tag{2.4}$$

where $\rho(x) = \displaystyle\sum_{i=1}^{N} |u_i(x)|^2$ is the electron density, $V_H(\rho) = \frac{1}{2}\int_{\mathbb{R}^3} \frac{\rho(y)}{|x-y|} dy$ denotes the Hartree potential, $V_{\text{xc}}(\rho)$ indicates the exchange-correlation potential, and $V_{\text{ext}}(x)$ is the electrostatic potential generated by the nuclei, including both full-potentials and pseudopotential approximations. For full-potentials, $N = N_e$ and $V_{\text{ext}}(x) = -\displaystyle\sum_{k=1}^{M} \frac{Z_k}{|x - \mathbf{R}_k|}$. While for pseudopotential approximations, N equals to the number of valence electrons, $V_{\text{ext}} = V_{\text{loc}} + V_{\text{nl}}$, with V_{loc} being the local part of pseudopotential and V_{nl} being a nonlocal part given by (see, e.g., [23])

$$V_{\text{nl}}\phi = \sum_{j=1}^{n} (\phi, \zeta_j)\zeta_j$$

with $n \in \mathbb{N}$ and $\zeta_j \in L^2(\Omega) (j = 1, 2, \cdots, n)$.

By density functional theory (DFT) [17, 19](see, also, [23, 25]), the ground state (charge) density of the system may be obtained by solving the lowest N eigenpairs of (2.4). In computation, $V_H(\rho)$ is usually obtained by solving the following Poisson equation:

$$-\Delta V_H(\rho) = 4\pi\rho(x). \tag{2.5}$$

The exact formula for exchange-correlation potential V_{xc} is unknown. Some approximation (such as LDA, GGA) has to be used.

Note that the ground state wavefunction of the Schrödinger equation and the solutions of Kohn-Sham model are exponentially decay [2, 3, 30], $\mathbb{R}^3$ is then replaced by some polyhedral domain $\Omega \subset \mathbb{R}^3$ in computation. Instead of (2.4), more precisely, we solve

$$\left\{ \begin{array}{rcl} a(U;u_i,v) & = & \lambda_i\big(u_i,v\big) \quad \forall\ v \in H_0^1(\Omega), \\ \displaystyle\int_\Omega u_i u_j & = & \delta_{ij}, \quad i,j = 1,2,\cdots,N, \end{array} \right. \tag{2.6}$$

where $U = (u_1, u_2, \cdots, u_N)$ and $a(U;\cdot,\cdot) : H_0^1(\Omega) \times H_0^1(\Omega) \to \mathbb{R}$ is defined by

$$a(U;w,v) = \frac{1}{2}(\nabla w, \nabla v) + ((V_{\rm ext} + V_H(\rho) + V_{xc}(\rho_{_U}))w, v) \quad \forall\ w, v \in H_0^1(\Omega) \tag{2.7}$$

with $\rho_{_U} = \displaystyle\sum_{i=1}^{N} |u_i|^2$.

3. Parallel orbital-updating algorithm. In this section, we shall introduce the parallel orbital-updating algorithm for the Kohn-Sham equation. Obviously, the same idea can be applied to solve Hartree-Fock equations as well as other eigenvalue problems.

3.1. Finite dimensional discretization. Consider a finite dimensional discretization of (2.6) as follows:

$$\left\{ \begin{array}{rcl} a(U_n;u_{n,i},v_n) & = & \big(\lambda_{n,i}u_{n,i},v_n\big) \quad \forall\ v_n \in V_n, \\ \displaystyle\int_\Omega u_{n,i}u_{n,j} & = & \delta_{ij}, \quad i,j = 1,2,\cdots,N, \end{array} \right. \tag{3.1}$$

where V_n is some finite dimensional space. We see that (3.1) is a nonlinear eigenvalue problem, and the so called self-consistent field (SCF)(see, e.g., [20, 24]) iteration approaches are often used to linearize it.

We may divide the finite dimensional discretizations for Kohn-Sham equations into three classes: the plane wave method, the local basis set method, and the real space method. The plane wave method uses plane wave functions as the basis functions to span a finite dimensional space V_n, while the local basis set method uses some Slater type or Gaussian type functions as the bases to construct a finite dimensional space V_n. The finite element method is one of commonly used real space methods, where finite element bases are used to construct V_n. No matter what kind of methods are used to discretize the Kohn-Sham equation, after linearization, what we get is some algebraic eigenvalue problem $Au = \lambda Bu$, where A is the stiff matrix, B is the mass matrix. And we need to solve the first N eigenvalues and the corresponding eigenfunctions of the algebraic eigenvalue problem. If A and B are sparse, e.g., discretized by a finite element method, then the optimal computational complexity is $\mathcal{O}(N^2N_g)$, while if A or B is dense, e.g., discretized by a plane wave method or a local basis set method, then the optimal computational complexity becomes $\mathcal{O}(NN_g^2)$. Here, N_g is the dimension of the matrix. We see that $N_g \gg N$ or a practically complete basis set is difficult to obtain. Note that to obtain an accurate approximation, one needs to solve tens of such algebraic eigenvalue problems, which limits the application of Kohn-Sham DFT to large scale systems, especially for full-potential calculations.

3.2. Parallel orbital-updating approach. We have already seen that the huge computational complexity for solving the discretized eigenvalue problems limits the application of Kohn-Sham DFT to the electronic structure calculations for large scale systems. Hence, a faster, accurate and efficient algorithm for solving Kohn-Sham equations as well as other eigenvalue problems is desired. In this subsection, we propose some new approach that can reduce the computational complexity remarkably, as compared with the existing methods of solving Kohn-Sham equations.

We understand that the Kohn-Sham equation is established within the framework of single-particle approximation, and can be viewed as a set of single-particle equations of independent particles that move in an effective potential. Motivated by the setting that independent particle moves in an efficient potential, we are indeed able to carry out these single-particle orbitals individually or in parallel intrinsically. It is shown by our investigation that a simple iteration with some observational data would be efficient for a special situation and supercomputers.

We note that for solving a large scale eigenvalue problem, an iteration scheme is usually used, which can also be view as (a discretized version of) some motion. Based on our understanding that the basic rule of motion is simple but the initial data may be special, we propose the following parallel orbital-updating algorithm for solving the Kohn-Sham equation based on finite element discretizations.

ALGORITHM 3.1.

1. *Given initial data* $(\lambda_i^{(0)}, u_i^{(0)}) \in \mathbb{R}\times H_0^1(\Omega)$ *with* $\|u_i^{(0)}\|_{0,\Omega} = 1 (i = 1, 2, \cdots, N)$, *define* $\mathcal{T}_0$ *and* V_0, *and let* $n = 0$
2. *Construct* $\mathcal{T}_{n+1}$ *and* V_{n+1} *based on an adaptive procedure to* $(\lambda_i^{(n)}, u_i^{(n)})$.
3. *For* $i = 1, 2, \cdots, N$, *find* $u_i^{(n+1/2)} \in V_{n+1}$ *satisfying*

$$a(U^{(n)}; u_i^{(n+1/2)}, v) = \lambda_i^{(n)}(u_i^{(n)}, v) \ \forall v \in V_{n+1} \tag{3.2}$$

   in parallel.
4. *Project to eigenspace: find* $(\lambda^{(n+1)}, u^{(n+1)}) \in \mathbb{R}\times\tilde{V}_{n+1}$ *satisfying* $\|u^{(n+1)}\|_{0,\Omega} = 1$ *and*

$$a(U^{(n+1/2)}; u^{(n+1)}, v) = \lambda^{(n+1)}(u^{(n+1)}, v) \quad \forall v \in \tilde{V}_{n+1} \tag{3.3}$$

   to obtain eigenpairs $(\lambda_i^{(n+1)}, u_i^{(n+1)})(i = 1, 2, \cdots, N)$.
5. *Let* $n = n + 1$ *and go to Step 2.*

Here $\tilde{V}_{n+1} = \ span\ \{u_1^{(n+1/2)}, u_2^{(n+1/2)}, \cdots, u_N^{(n+1/2)}\}$, $U^{(n)} = (u_1^{(n)}, u_2^{(n)}, \cdots, u_N^{(n)})$, *and* $U^{(n+1/2)} = (u_1^{(n+1/2)}, u_2^{(n+1/2)}, \cdots, u_N^{(n+1/2)})$.

In our computation in Section 4, we choose V_n as some finite element space $S_0^{h_n,k}(\Omega)$ over $\mathcal{T}_n$ with some k, the degree of piecewise polynomials. While $\mathcal{T}_n$ is constructed based on some a posteriori error estimations of $(\lambda_i^{(n)}, u_i^{(n)})$, marking strategy and refine procedure as described in Section 2.1. Indeed, V_n can also be any other appropriate relevant finite dimensional spaces.

We see that to provide a physical observational data is natural and significant for algorithm's efficiency. In electronic structure calculations, we may choose the initial data $(\lambda_i^{(0)}, u_i^{(0)})$ as follows:

- Gaussian-type orbital or Slater-type orbital based guesses, which are applicable to full-potential calculations,
- local plane-wave discretization based guesses, which are applicable to pseudopotential settings,

- local finite element/volume discretization based guesses (c.f., e.g.,[9, 10, 11, 13]), which are applicable to either full-potential calculations or pseudo-potential settings.

It will be demonstrated by our experiments in Section 4 that the parallel orbital-updating approach is powerful in electronic structure calculations. Here we mention several features of Algorithm 3.1 as follows:

- **Model linearization**. We understand from Algorithm 3.1 that our parallel orbital-updating approach is in fact some new SCF iteration technique and mixes simple discretization iterations of source problems with adaptive computations.
- **Complexity reduction**. We see form our new algorithm that the solution of the original tens of large scale eigenvalue problems is reduced to the solution of some independent source problems and some small scale eigenvalue problems. Since these source problems are independent each other, our parallel orbital-updating algorithm can be carried out in parallel intrinsically. Indeed, the computational complexity then becomes $\mathcal{O}(N_g + N_{orb}^3)$, which is much lower than $\mathcal{O}(N_{orb}^2 N_g)$ or $\mathcal{O}(N_{orb} N_g^2)$, the costs for solving the Kohn-Sham equation directly, where N_{orb} is the number of desired eigenvalues and N_g is the number of unknowns of the discretized Kohn-Sham equation or the dimension of the resulting matrix.
- **Eigenvalue separation**. If the initial guess is well-posed, then we are able to obtain the orbital approximations individually. For illustration, we comment the more general setting Algorithm A.1 rather than Algorithm 3.1, which is applied to solve eigenvalue problem (A.3).
  For $\lambda \in \sigma(L)$, define
  $$\delta(\lambda) = \inf\{\|w - v\|_{l,\Omega} : w \in M(\lambda), v \in M(\mu), \mu \in \sigma(L) \setminus \{\lambda\}\}.$$
  Let $\mu_i \in \sigma(L)$ whose multiplicity is $q_i (i = 1, 2, \cdots, M)$, respectively[1]. Assume that the initial data $(\lambda_{i+j}^{(0)}, u_{i+j}^{(0)}) \in \mathbb{R} \times H_0^1(\Omega)$ satisfying that $\|u_{i+j}^{(0)}\|_{0,\Omega} = 1 (i = 1, 2, \cdots, M; j = 0, 1, 2, \cdots, q_i - 1)$ and $\text{span}\{u_{i+j}^{(0)} : j = 0, 1, 2, \cdots, q_i - 1\}$ away from
  $$\cup \{M(\mu) : \mu \in \sigma(L) \setminus \{\mu_i\}\}, \ i = 1, 2, \cdots, M.$$
  More precisely, for $i = 1, 2, \cdots, M$,
  $$\inf\{\|u_{i+j}^{(0)} - v\|_{0,\Omega} : j = 0, 1, 2, \cdots, q_i - 1; v \in M(\mu), \mu \in \sigma(L) \setminus \{\mu_i\}\} > \delta(\mu_i)/2.$$
  Then we may apply Algorithm A.1 to obtain eigenspace approximations in parallel. We observe that the computational cost
  $$\mathcal{O}\left(\left(\sum_{i=1}^{M} q_i\right)^3\right)$$
  of computing eigenpairs is then reduced to
  $$\mathcal{O}\left(\sum_{i=1}^{M} q_i^3\right).$$

[1] In our discussion, $q_1 = 1$ when $\mu_1 = \lambda_1$.

- **Two-level parallelization**. We may also see a potential of our algorithm in large scale parallel computation. Since these source problems are independent each other, they can be calculated in parallel intrinsically, and each source problems can also be solved in parallel by various multigrid or domain decomposition approaches, which is a two level parallelization. One level is the solution of these N independent source problems in parallel intrinsically, another level is to solve each source problem in parallel by using idea of multigrid or domain decomposition methods. As a result, there may be some potential for E-scale eigenvalue computations.

We point out that if the initial guess is not well-provided, then we suggest to apply the following algorithm:

ALGORITHM 3.2.

1. *Given initial data* $(\lambda_i^{(0)}, u_i^{(0)}) \in \mathbb{R}\times H_0^1(\Omega)$ *with* $\|u_i^{(0)}\|_{0,\Omega} = 1 (i = 1, 2, \cdots, N+m)$, *define* $\mathcal{T}_0$ *and* V_0, *and let* $n = 0$
2. *Construct* $\mathcal{T}_{n+1}$ *and* V_{n+1} *based on an adaptive procedure to* $(\lambda_i^{(n)}, u_i^{(n)})$.
3. *For* $i = 1, 2, \cdots, N+m$, *find* $u_i^{(n+1/2)} \in V_{n+1}$ *satisfying*

$$a(U^{(n)}; u_i^{(n+1/2)}, v) = \lambda_i^{(n)}(u_i^{(n)}, v)\ \forall v \in V_{n+1}$$

   in parallel.
4. *Project to eigenspace: find* $(\lambda^{(n+1)}, u^{(n+1)}) \in \mathbb{R}\times\tilde{V}_{n+1}$ *satisfying* $\|u^{(n+1)}\|_{0,\Omega} = 1$ *and*

$$a(U^{(n+1)}; u^{(n+1)}, v) = \lambda^{(n+1)}(u^{(n+1)}, v) \quad \forall v \in \tilde{V}_{n+1}$$

   to obtain eigenpairs $(\lambda_i^{(n+1)}, u_i^{(n+1)}) (i = 1, 2, \cdots, N+m)$.
5. *Let* $n = n+1$ *and go to Step 2.*

Here $\tilde{V}_{n+1} = \ span\ \{u_1^{(n+1/2)}, u_2^{(n+1/2)}, \cdots, u_{N+m}^{(n+1/2)}\}$, $U^{(n)} = (u_1^{(n)}, u_2^{(n)}, \cdots, u_N^{(n)})$, $U^{(n+1/2)} = (u_1^{(n+1/2)}, u_2^{(n+1/2)}, \cdots, u_N^{(n+1/2)})$, *and* m *is some proper integer.*

It tells from Algorithm 3.2 that more eigenpairs should be computed so as to get a better approximation of the first N orbitals. In practice, we see that Algorithm 3.2 is more stable than Algorithm 3.1.

We may refer to Appendix for a generalization to a class of linear eigenvalue problems and its basic numerical analysis.

4. Numerical experiments. In this section, we apply our parallel orbital-updating algorithm based on finite element discretizations to simulate several typical molecular systems: H_2O(water), $C_9H_8O_4$(aspirin), $C_5H_9O_2N$(α amino acid), $C_{17}H_{19}N_3$(mirtazapine), $C_{20}H_{14}N_4$(porphyrin), and C_{60}(fullerene), to show the reliability and efficiency of our approach. Due to the length limitation of the paper, we only show the results for full potential calculations for illustration.

We understand that Gaussian[16] is a popular and widely used electronic structure package. In Gaussian09, many different basis sets with different level of accuracy are provided for the DFT approach, for example, STO-3G, STO-6G, 6-31G, cc-pVDZ, cc-pVTZ, cc-pVQZ, cc-pV5Z, cc-pV6Z, and others. The better the accuracy, the larger the cpu time cost.

To show the efficiency of our algorithm, we compare our results with the results obtained by Gaussian09 [16] within the LDA81 DFT setting [26] and using bases 6-31G, cc-pVQZ, cc-pV5Z as well as cc-pV6Z, respectively. In our computation, we use

also LDA81 as the exchange correlation functional and apply the STO-3G basis to obtain the initial guess in Algorithm 3.1.

Both the results obtained by our algorithm and those obtained by Gaussian09 are carried out on LSSC-III in the State Key Laboratory of Scientific and Engineering Computing, Chinese Academy of Sciences, and our package RealSPACES (Real Space Parallel Adaptive Calculation of Electronic Structure) that are based on the toolbox PHG [27] of the State Key Laboratory of Scientific and Engineering Computing, Chinese Academy of Sciences. All results are given by atomic units (a.u.).

In our tables, we use some abbreviations:

- ParO =Parallel orbital-updating approach
- MeshG =Mesh generation
- SourceS =Source problem solution
- DOFs=Degrees of freedom
- N_{procs}=Number of processors

4.1. Validation of reliability. First, we will validate the reliability of our algorithm by using a small molecular system as example. As well known, for small atomic or molecular systems, Gaussian09 provides very efficient and accurate results To illustrate the reliability of our algorithm, we use H_2O as an example to show that the results obtained by our algorithm are reliable by comparing with those obtained by Gaussian09.

Example 1: H_2O

The atomic configuration for molecule H_2O is figured in Fig. 4.1. Here we compute the first 5 eigenpairs of the associated Kohn-Sham equation.

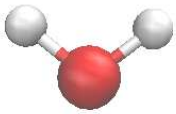

FIG. 4.1. *Configuration of* H_2O *(*$N_{orb} = 5$*)*

Table 1 provides the detailed information for results obtained by Gaussian09 with different kinds of basis functions being used and those obtained by our algorithm after different number of iterations. The second column is the total energy obtained, the third column is the number of basis functions used, the forth column is the wall-time cost, while the fifth column is the number of processors used.

It should be pointed out that in our current numerical experiments, the N_{orb} number of boundary value problems are solved one by one, not in parallel, and here the multi processors deal with only the parallelization in space, not in orbital. That is, the N_{orb} boundary value problems (3.2) are solved one by one, not in parallel. If we have enough processors, the N_{orb} boundary value problems can be carried out in parallel intrinsically, the wall-time cost by our algorithm would be reduced further, and it is listed in the last column with color red.

Method	E_{tot}(a.u.)	DOFs	Time(s)	N_{procs}	Time(s)
STO-3G	−74.729534	7	1	1	–
STO-6G	−75.446932	7	2	1	–
6-31G	−75.814098	13	2	1	–
cc-pVDZ	−75.850750	24	3	1	–
cc-pVTZ	−75.894284	58	3	1	–
cc-pVQZ	−75.904123	115	5	1	–
cc-pV5Z	−75.908214	201	23	1	–
cc-pV6Z	−75.909024	322	1111	1	–
ParO (116)	−75.908257	594027	1096.8	32	939.5
ParO (149)	−75.909026	1253803	2863.6	32	2399.4
ParO (166)	−75.909175	2007831	4654.6	32	3845.4

TABLE 1
Results of H_2O

We observe from Table 1 that for Gaussian09, as the bases changes from STO-3G to cc-pV6Z, the total ground state energy approximation reduces from large to small, while the corresponding cpu-time cost increases fastly, especially when the ground state energy approximation is closed to the exact one. For example, when using bases from cc-pV5Z to cc-pV6Z, the total energy decreases about 0.00081 a.u., while the cpu-time cost increases 1088s. More precisely, for the basis set method, the cost is not expensive if only less accurate result is required, while the cost will become very huge if the the accuracy of approximation increases a little bit after some critical accuracy.

We see that the ground state energy approximations obtained by our algorithm after 116 iterations(here, 1 iteration means doing Step 2, Step 3, and Step 4 of Algorithm 3.1 once) is −75.908257 a.u., which is very close to that obtained by Gaussian09 using basis cc-pV5Z, and if we refine the mesh adaptively and do one iteration again , then the ground state energy approximation will decrease further. Let us take a more detailed. After 149 iterations, the energy approximation decreases to −75.909026 a.u., close to the results obtained by Gaussian09 using basis cc-pV6Z. If we do more iterations, that is, after 166 iterations, the energy approximation decreases to −75.909175 a.u., smaller than that obtained by Gaussian09 using basis cc-pV6Z by 0.000151 a.u..

Although the total cpu time cost by our algorithm is much longer than that cost by Gaussian09, we should note that the cpu-time cost does not increase as quickly as that for Gaussian09. In fact, for Gaussian09, when the bases are chosen from cc-pV5Z to cc-pV6Z, the total energy approximation decreases from −75.908214 a.u. to −75.909024 a.u., the cpu-time cost increases from 23s to 1111s, about 50 times of the former one. For our algorithm, from 116 iterations to 149 iterations, the energy approximation decreases from −75.908257 a.u. to −75.909026 a.u., the cpu-time cost increases from 1096.8s to 2863.6s, only about 3 times of the former one.

Fig. 4.2 shows the convergence curve for the ground state energy approximations over each adaptive refined mesh, where the x-axis is the DOFs, and the y-axis is the ground state energy approximation. We see from Fig. 4.2 that the total energy approximation converges as the number of degrees increases. For comparison, we show the convergence curve of the total energy obtained by Gaussian09 with different kinds of bases(STO-3G, STO-6G, 6-31G, cc-pVDZ, cc-pVTZ, cc-pVQZ, cc-pV5Z, cc-pV6Z from the right to the left) in Fig. 4.3.

We may conclude that our algorithm can produce approximations as accurate

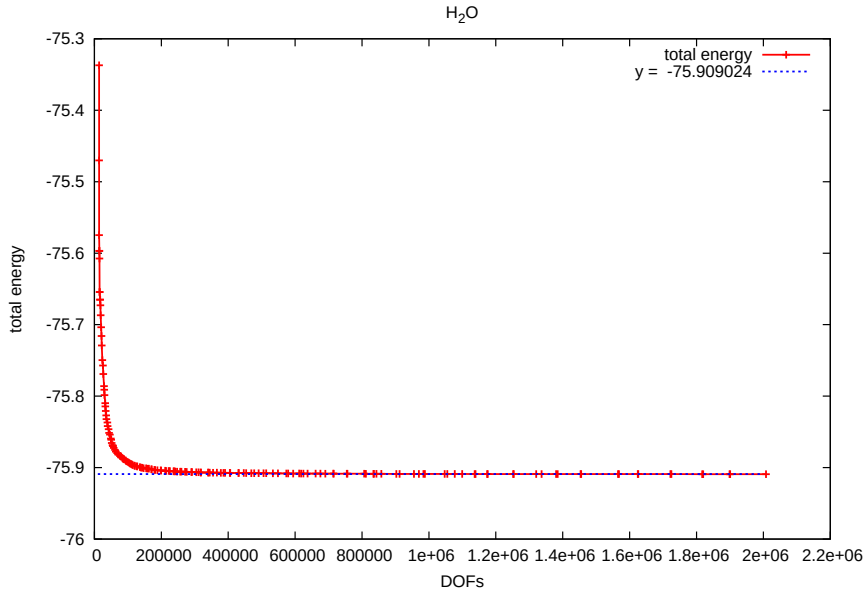

FIG. 4.2. *Convergence curves of the ground state energy*

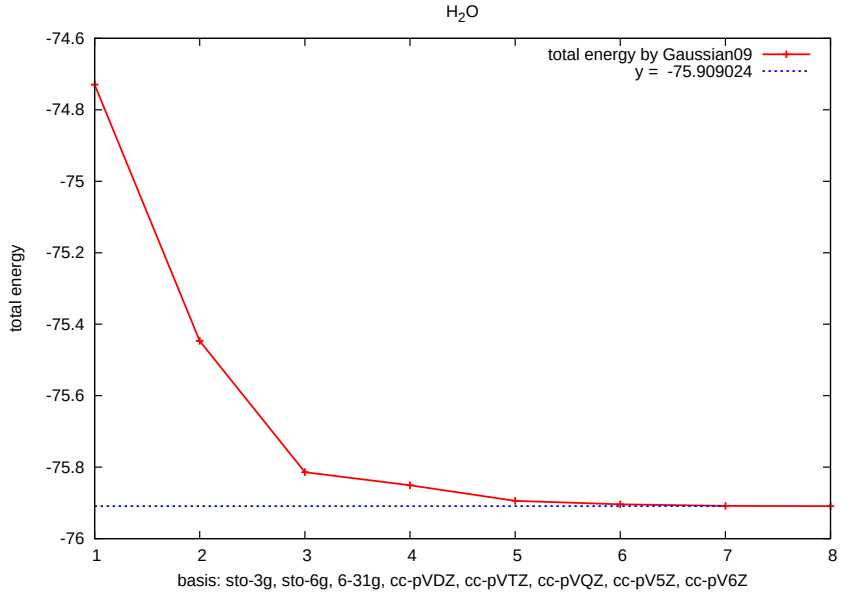

FIG. 4.3. *Convergence curves of ground state energy by Gaussian09*

as or even more accurate than Gaussian09. Although for such a small example, the cpu-time cost by our algorithm is much longer than that cost by Gaussian09, we can see the potential of our algorithm when highly accurate results are desired.

4.2. Validation of efficiency. Although Gaussian09 can provide highly accurate results quickly for small molecular systems, it is another story for molecular systems of medium or large size. We see that the memory required for DFT method scales as N^4 with N being the number of basis functions, for instance.

In this subsection, we will use some molecular systems of medium scale or large scale to show the efficiency of our algorithm.

Example 2: α-amino acid: $C_5H_9O_2N$

The atomic configuration for molecule $C_5H_9O_2N$ is shown in Fig. 4.4. For this example, we compute the first 31 eigenpairs of the Kohn-Sham equation, and 32 processors are used for both Gaussian09 and our code. Table 2 displays the relevant results.

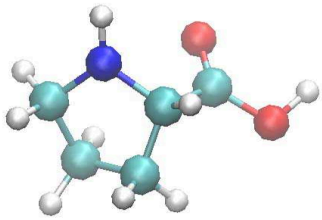

FIG. 4.4. *Configuration of* $C_5H_9O_2N$ *(*$N_{orb} = 31$*)*

Method	E_{tot}(a.u.)	DOFs	Time(s)	N_{procs}	Time(s)
STO-3G	−392.621189	49	2.9	32	–
6-31G	−397.673071	90	3.3	32	–
cc-pVQZ	−397.998732	710	386.7	32	–
cc-pV5Z	−398.009882	1223	2444.6	32	–
ParO (127)	−398.009800	3605766	19771.6	32	8708.8
ParO (136)	−398.010611	4634263	28868.7	32	12101.5
MeshG	−392.630620	104037	4.5		4.5
SourceS	−398.010611	4634263	17131.7	32	364.5

TABLE 2
Results of $C_5H_9O_2N$

We see from Table 2 that the total energy approximation obtained by Gaussian09 decreases when the bases are chosen from STO-3G to cc-pV5Z, while the cpu-time cost increases quickly. We mention that due to the huge storage requirement, we are not able to produce the result by Gassian09 using bases cc-pV6Z.

We also observe from Table 2 that after 127 iterations, the total ground state energy approximations obtained by our algorithm is −398.009800a.u., which is close to that obtained by cc-pV5Z. If we refine the mesh adaptively again, we can obtain more accurate results. For example, after 136 iterations, the total energy approximation decreases to −398.010611a.u., which is 0.000729a.u. smaller than that obtained

by Gassian09 using bases cc-pV5Z. The cpu-time cost after 127 iterations and 136 iterations are about 19771.6s and 28868.7s respectively. As we addressed in **Example 1**, in our current computations, the N_{orb} number of boundary value problems are solved one by one, not in parallel, and here the 32 processors deal with only the parallelization in space, not in orbital. Since the 31 boundary value problems can be carried out in parallel intrinsically, the wall-time cost by our algorithm cost would be at least reduced to 8708.8s and 12101.5s respectively provided we have $992(32 \times 31)$ processors.

We note from Fig. 4.5 that the total energy approximation converges as the iteration increases.

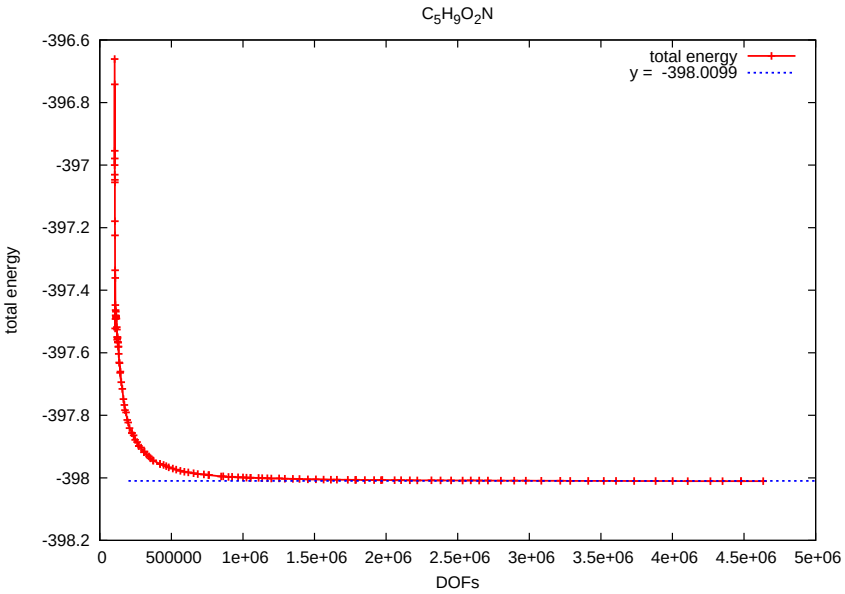

FIG. 4.5. *Convergence curves of the ground state energy*

Example 3: $C_9H_8O_4$

The atomic configuration for molecule $C_9H_8O_4$ is shown in Fig. 4.6. We solve the first 47 eigenpairs of the Kohn-Sham equation.

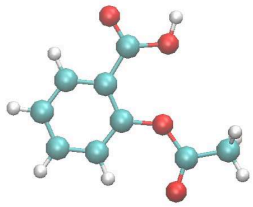

FIG. 4.6. *Configuration of* $C_9H_8O_4$ *(*$N_{orb} = 47$*)*

Table 3 digitizes some relevant results, including those obtained by Gaussian09 and those obtained by our algorithm over the mesh got by 79 adaptive refinements.

Fig. 4.7 displays the convergence curve of the ground state energy approximation over each adaptive refined mesh.

Method	E_{tot}(a.u.)	DOFs	Time(s)	N_{procs}	Time(s)
STO-3G	−634.903702	73	4.2	32	–
6-31G	−643.159782	133	10.7	32	–
cc-pVQZ	−643.656111	955	895.8	32	–
cc-pV5Z	−643.673930	1623	3782.8	32	–
ParO (91)	−643.648898	10983675	41390.8	32	23229.7
MeshG	−635.473477	609169	48.1		48.1
SourceS	−643.648898	10983675	18555.9	32	394.8

TABLE 3
Results of $C_9H_8O_4$

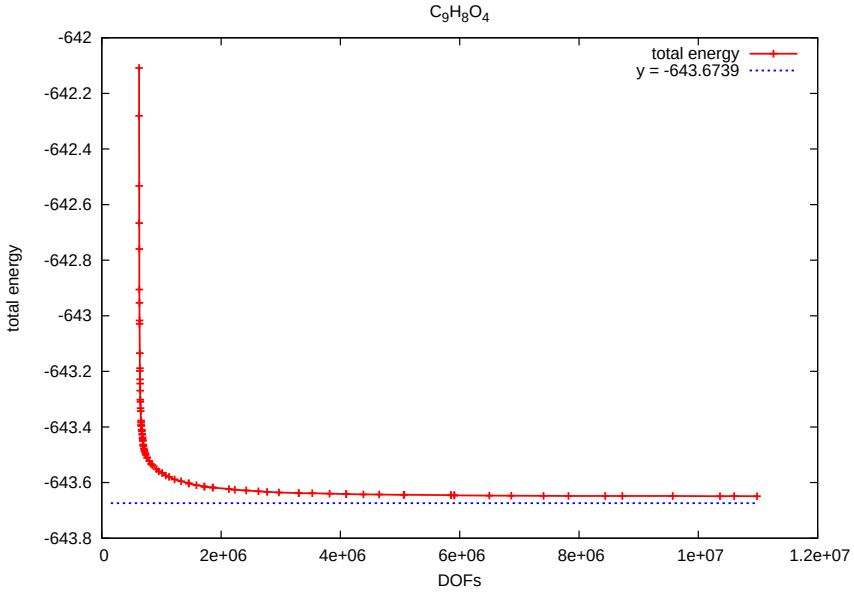

FIG. 4.7. *Convergence curves of the ground state energy*

For this example, the total energy obtained by our algorithm are a little larger than that obtained by Gaussian09 with cc-pV5Z being used.

4.3. Full-potential calculation for large scale system. In this subsection, we apply our algorithm to full-potential electronic structure calculations for some large molecular systems.

Example 4: $C_{17}H_{19}N_3$

The configuration for molecule $C_{17}H_{19}N_3$ is shown in Fig. 4.8 and the first 71 eigenpairs of the Kohn-Sham equation are computed, and 32 processors are used for both Gaussian09 and our code. Table 4 provides the relevant results.

We observe from Table 4 that after 73 iterations, the total energy obtained by our algorithm is very close to that obtained by Gaussian09 with using bases cc-pV5Z. Let us take a look at the cpu-time cost. We see that when using the same number

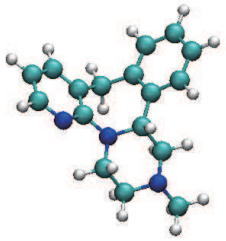

FIG. 4.8. *Configuration of* $C_{17}H_{19}N_3$ *(*$N_{orb} = 71$*)*

Method	E_{tot}(a.u.)	DOFs	Time(s)	N_{procs}	Time(s)
STO-3G	−805.972579	119	4.3	32	–
6-31G	−815.869313	218	19.9	32	–
cc-pVQZ	−816.445414	1670	3456.6	32	–
cc-pV5Z	−816.467053	2865	20675.6	32	–
ParO (73)	−816.468992	6007146	33416.7	32	13885.0
ParO (91)	−816.493475	9963665	86465.1	32	31137.4
MeshG	−805.778326	264415	31.2		31.2
SourceS	−816.493475	9963665	56118.1	32	790.4

TABLE 4
Results of $C_{17}H_{19}N_3$

of processors, the cpu-time cost by Gaussian09 and our algorithm are 20675.6s and 33416.7s, respectively. Note that the N_{orb} boundary value problems are solved one by one, not in parallel. If we apply $2272(= 32 \times 71)$ processors, indeed, the cpu-time cost by our algorithm can then be reduced to 13885.0s. If we refine the mesh again, the energy approximation will reduce further. For instance, after 91 iterations, the total energy approximation will reduce to −816.493475, which is 0.026422 a.u. smaller than that obtained by Gaussian09 with cc-pV5Z being used.

Fig. 4.9 shows the convergence curve of the ground state energy approximation, from which we conclude that the approximation results obtained by our algorithm converge.

Example 5: $C_{20}H_{14}N_4$

The atomic configuration for molecule $C_{20}H_{14}N_4$ is shown in Fig. 4.10 and the first 81 eigenpairs of the Kohn-Sham equation are approximated.

Table 5 digitizes the computational results, including those obtained by Gaussian09 and those obtained by our algorithm after 58 and 68 iterations. Fig. 4.11 shows the convergence curve of the ground state energy. We get the similar conclusions as that obtained of **Example 4** from Table 5 and Fig.4.11.

Example 6: C_{60}

The atomic configuration for molecule C_{60} is shown in Fig. 4.12 and we compute the first 180 eigenpairs of the Kohn-Sham equation.

Table 6 digitizes the relevant data. Fig. 4.13 provides the convergence curves of the total energy after each iteration.

We conclude from Table 6 and Fig. 4.13 that the similar conclusions as that of **Example 4** can be obtained.

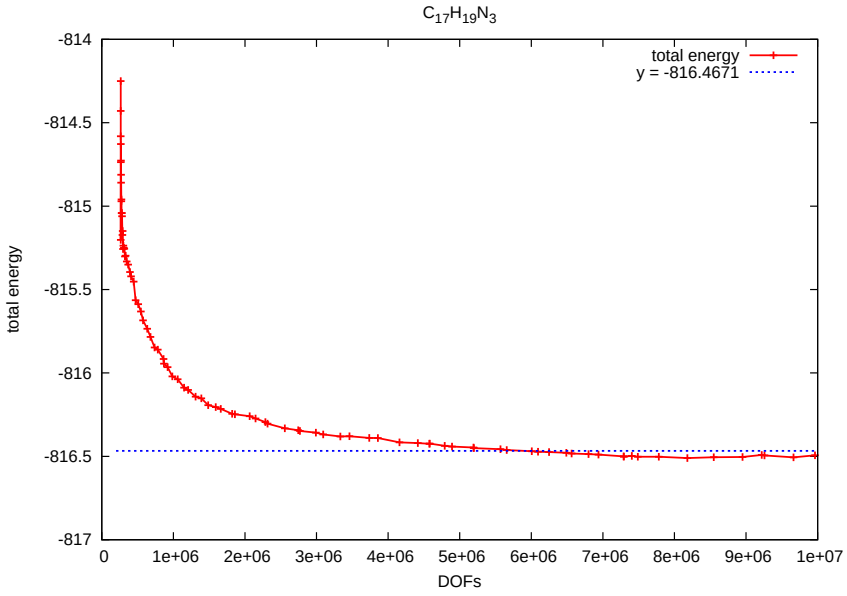

FIG. 4.9. *Convergence curves of the ground state energy*

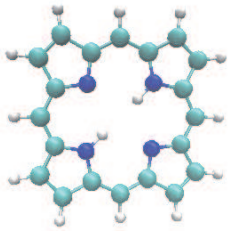

FIG. 4.10. *Configuration of* $C_{20}H_{14}N_4$ *(*$N_{orb} = 81$*)*

5. Concluding remarks. In this paper, we proposed a parallel orbital-updating algorithm for electronic structure calculations, which are demonstrated to be accurate and efficient for full-potential calculations based on finite element discretizations.

From the comparison between results obtained by our algorithm and those obtained by Gaussian 09 with different kinds of basis sets, we may conclude that

- our algorithm can produce highly accurate approximations to the exact one for medium or large scale systems;
- the cpu time cost by our algorithm is much lower than that cost by Gaussian09, especially for large scale systems;
- our algorithm are efficient for full-potential calculations for large scale systems;
- our algorithm is sequential parallel, which may mean that it has a potential to supercomputing.

Although we have a primitive analysis as Theorem A.1, we are currently not able to present a mathematically rigorous proof how the approximations converge to

Method	E_{tot}(a.u.)	DOFs	Time(s)	N_{procs}	Time(s)
STO-3G	−968.459221	134	3.9	32	–
6-31G	−980.529009	244	12.4	32	–
cc-pVQZ	−981.230600	1710	1798.7	32	–
cc-pV5Z	−981.257126	2954	10499.2	32	–
ParO (58)	−981.257001	5861789	30109.6	32	11738.6
ParO (68)	−981.270015	10219345	77275.6	32	25223.8
MeshG	−965.172827	596951	40.9		40.9
SourceS	−981.270015	10219345	52702.5	32	650.6

TABLE 5
Results of $C_{20}H_{14}N_4$

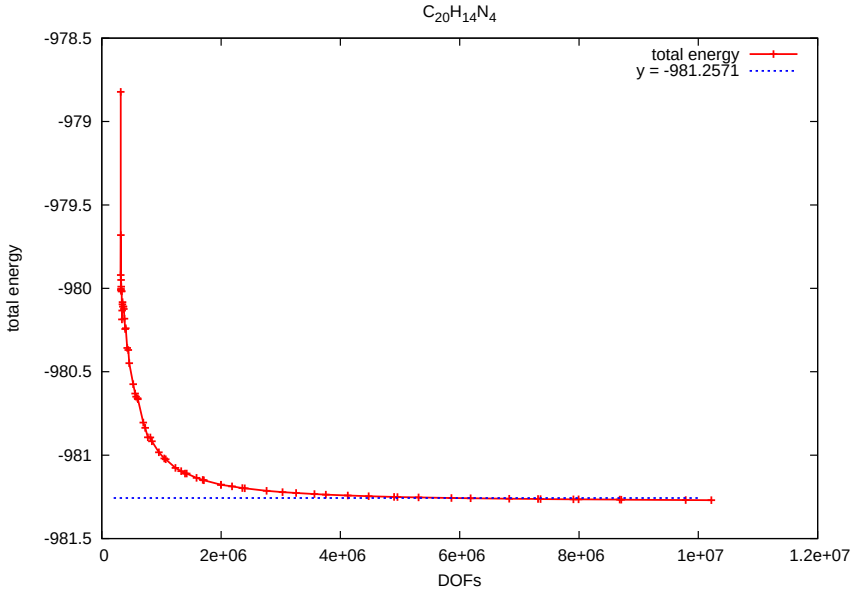

FIG. 4.11. *Convergence curves of the ground state energy*

the exact ground state energy and density. Note that only simple and basic source problems have been employed in our algorithms. It is our on-going work to study and apply more efficient source models into our parallel orbital-updating approach to speed up the approximation convergence, which will be addressed elsewhere. Anyway, we believe that our approach is a general and powerful parallel-computing technique that can be applied to a variety of eigenvalue problems, including partial differential equation based ones with differential types of discretization methods, and other nonlinear problems.

Acknowledgements. The authors would like to thank Doctor Hongping Li his helps in using Gaussian09.

Appendix: Parallel orbital-updating algorithm for linear eigenvalue problems. In this appendix, we show that the parallel orbital-updating approach can be applied to a general eigenvalue computation.

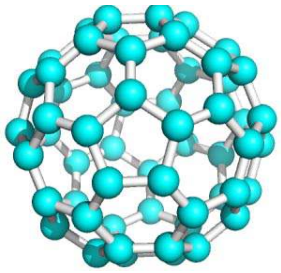

FIG. 4.12. *Configuration of* C_{60} $(N_{orb} = 180)$

Method	E_{tot}(a.u.)	DOFs	Time(s)	N_{procs}	Time(s)
STO-3G	−2238.127540	300	80.5	64	–
6-31G	−2265.319422	540	102.1	64	–
cc-pVQZ	−2266.766797	3300	6250.3	64	–
cc-pV5Z	−2266.824090	5460	53034.7	64	–
ParO (88)	−2266.820160	10742296	88894.4	64	38533.2
ParO (95)	−2266.837443	13425339	137958.4	64	55662.4
MeshG	−2239.762286	596951	174.5		174.5
SourceS	−2266.837443	13425339	51188.3	64	410.3

TABLE 6
Results of C_{60}

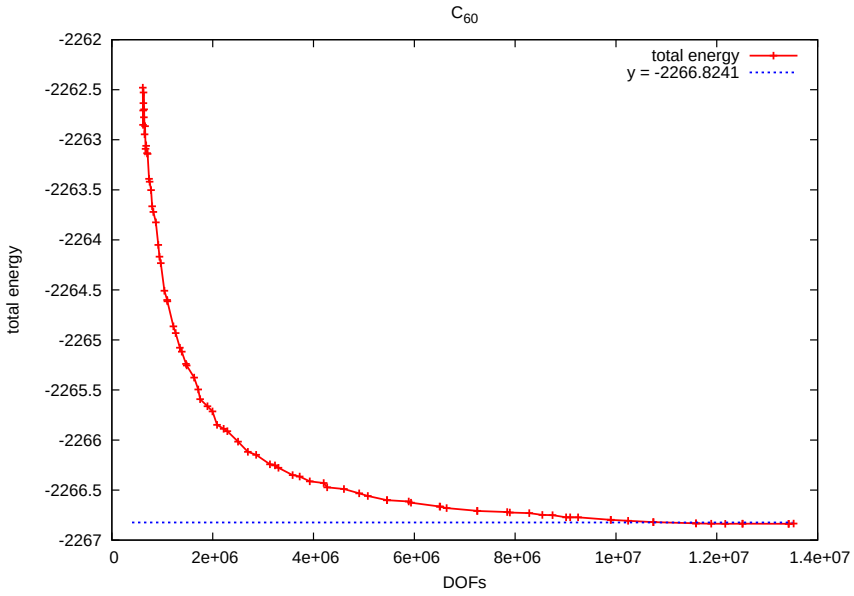

FIG. 4.13. *Convergence curves of the ground state energy*

Consider eigenvalue problem:

$$\text{(A.1)} \qquad \begin{cases} Lu &= \lambda u \text{ in } \Omega, \\ u &= 0 \text{ on } \partial\Omega, \end{cases}$$

where L is a linear second order elliptic operator:

$$Lu = -\nabla \cdot (A\nabla u) + cu$$

with $A : \Omega \to \mathbb{R}^{d\times d}$ being piecewise Lipschitz with respect to the initial triangulation and symmetric positive definite with smallest eigenvalue uniformly bounded away from 0, and $0 \le c \in L^\infty(\Omega)$ [2].

Define

$$\text{(A.2)} \qquad a(u,v) = \int_\Omega A\nabla u\nabla v + cuv, \ \forall u, v \in H^1(\Omega).$$

The weak form of (A.1) can be written as follows: find a pair $(\lambda, u) \in \mathbb{R} \times H_0^1(\Omega)$ satisfying $\|u\|_{0,\Omega} = 1$ and

$$\text{(A.3)} \qquad a(u,v) = \lambda(u,v) \quad \forall v \in H_0^1(\Omega).$$

Equation (A.3) has a sequence of real eigenvalues $\sigma(L) \equiv \{\lambda_i : i = 1, 2, \cdots\}$:

$$0 < \lambda_1 < \lambda_2 \le \lambda_3 \le \cdots$$

and the corresponding eigenfunctions $u_1, u_2, u_3, \cdots$, satisfying

$$(u_i, u_j) = \delta_{ij}, \ i, j = 1, 2, \cdots,$$

where the λ_j's are repeated according to geometric multiplicity.

Let $\lambda \in \sigma(L)$ and $M(\lambda)$ denote the space of eigenfunctions corresponding to λ:

$$M(\lambda) = \{w \in H_0^1(\Omega) : w \text{ is an eigenvector of (A.3) corresponding to } \lambda\}.$$

A standard finite element approximation for (A.3) is: find a pair $(\lambda_h, u_h) \in \mathbb{R} \times V_h$ satisfying $\|u_h\|_{0,\Omega} = 1$ and

$$\text{(A.4)} \qquad a(u_h, v) = \lambda_h(u_h, v) \quad \forall v \in V_h.$$

We may order the eigenvalues of Let $(\lambda_{i,h}, u_{1,h})(i = 1, 2, \cdots, n_h \equiv \dim V_h)$ be the eigenpairs of (A.4) satisfying

$$b(u_{i,h}, u_{j,h}) = \delta_{ij}, \ i, j = 1, 2, \cdots, n_h.$$

We propose a parallel orbital-updating algorithm for solving (A.4) as follows:

ALGORITHM A.1.

1. *Given initial data* $(\lambda_i^{(0)}, u_i^{(0)}) \in \mathbb{R} \times H_0^1(\Omega)$ *with* $\|u_i^{(0)}\|_{0,\Omega} = 1 (i = 1, 2, \cdots, N)$ *and* $\mathcal{T}_0$*, and let* $n = 0$*.*
2. *Construct* $\mathcal{T}_{n+1}$ *and* V_{n+1} *based on an adaptive procedure to* $(\lambda_i^{(n)}, u_i^{(n)})$*.*

[2] We mention that the results obtained in this paper are also valid for a more general bilinear form $a(\cdot,\cdot)$ (c.f., e.g., Remark 2.9 in [12]).

3. *For* $i = 1, 2, \cdots, N$, *find* $u_i^{(n+1/2)} \in V_{n+1}$ *satisfying*

$$a(u_i^{(n+1/2)}, v) = \lambda_i^{(n)}(u_i^{(n)}, v) \ \forall v \in V_{n+1}$$

in parallel.

4. *Project to eigenspace: find* $(\lambda^{(n+1)}, u^{(n+1)}) \in \mathbb{R}\times\tilde{V}_{n+1}$ *satisfying* $\|u^{(n+1)}\|_{0,\Omega} = 1$ *and*

$$a(u^{(n+1)}, v) = \lambda^{(n+1)}(u^{(n+1)}, v) \quad \forall v \in \tilde{V}_{n+1}$$

to obtain eigenpairs $(\lambda_i^{(n+1)}, u_i^{(n+1)})(i = 1, 2, \cdots, N)$.

5. *Let* $n = n + 1$ *and go to Step 2.*

Here $\tilde{V}_{n+1} =$ *span* $\{u_1^{(n+1/2)}, u_2^{(n+1/2)}, \cdots, u_N^{(n+1/2)}\}$.

To analyze Algorithm A.1, we introduce a Galerkin-projection $P_h : H_0^1(\Omega) \to V_h \equiv S_0^h(\Omega)$ by

$$a(u - P_h u, v) = 0 \quad \forall u \in H_0^1(\Omega) \ \forall v \in V_h, \tag{A.5}$$

and apparently

$$\|P_h u\|_{1,\Omega} \lesssim \|u\|_{1,\Omega} \quad \forall u \in H_0^1(\Omega)$$

and

$$\|u - P_h u\|_{1,\Omega} \lesssim \inf_{v\in V_h} \|u - v\|_{1,\Omega} \quad \forall u \in H_0^1(\Omega).$$

THEOREM A.1. *Let* $(\lambda_i^{(1)}, u_i^{(1)})(i = 1, \cdots, N)$ *be obtained by Algorithm A.1 after one iteration,* $(\lambda_i, u_i)(i = 1, \cdots, N)$ *be the first* N *exact eigenpair of (A.3). Then*

$$d_1(u_i^{(1)}, V) \lesssim \sum_{k=1}^{N} \Big(|\lambda_k - \lambda_k^{(0)}| + \inf_{v\in V_1} \|u_k - v\|_1 + \|u_k - u_k^{(0)}\|_0\Big), \tag{A.6}$$

where $V = span\{u_1, \cdots, u_N\}$, *and the distance between* w *and* $W \in H_0^1(\Omega)$ *is defined by*

$$d_1(w, W) = \inf_{v\in W} \|w - v\|_{1,\Omega}. \tag{A.7}$$

Proof. Let $P_1 : H_0^1(\Omega) \longrightarrow V_1$ be the Galerkin projection defined by (A.5) when V_h is replaced by V_1. We see for any $u \in H_0^1(\Omega)$ that

$$a(P_1 u_i - u_i^{(1/2)}, v) = \lambda_i(u_i - u_i^{(0)}, v) + (\lambda_i - \lambda_i^{(0)})(u_i^{(0)} -, v) \ \ \forall v \in V_1,$$

which leads to

$$\|P_1 u_i - u_i^{(1/2)}\|_1 \lesssim \|u_i - u_i^{(0)}\|_0 + |\lambda_i - \lambda_i^{(0)}|.$$

We obtain from the triangle inequality that

$$\begin{aligned}\|u_i - u_i^{(1/2)}\|_1 &\lesssim \|u_i - P_1 u_i\|_1 + \|P_1 u_i - u_i^{(1/2)}\|_1 \\ &\lesssim \ \|u_i - P_1 u_i\|_1 + \|u_i - u_i^{(0)}\|_0 + |\lambda_i - \lambda_i^{(0)}|,\end{aligned}$$

where the first term on the right-hand side can be bounded by term $\inf_{v\in V_1}\|u_i-v\|_1$.

Since $u_i^{(1)} \in \tilde{V}_1 = span\{u_1^{(1/2)},\cdots,u_N^{(1/2)}\}$, we have that there exist constants $\alpha_{i,k}(k=1,\cdots,N)$, such that

$$u_i^{(1)} = \sum_{k=1}^{N} \alpha_{i,k} u_k^{(1/2)}.$$

Note that we may estimate as follows

$$\begin{aligned}\sum_{k=1}^{N}\alpha_{i,k}(u_k^{(1/2)}-u_k) &\lesssim \sum_{k=1}^{N}\alpha_{i,k}\Big(\|u_k-P_1u_k\|_1+\|u_k-u_k^{(0)}\|_0+|\lambda_k-\lambda_k^{(0)}|\Big)\\ &\lesssim \sum_{k=1}^{N}\Big(\|u_k-P_1u_k\|_1+\|u_k-u_k^{(0)}\|_0+|\lambda_k-\lambda_k^{(0)}|\Big).\end{aligned}$$

Consequently,

$$u_i^{(1)}-\sum_{k=1}^{N}\alpha_{i,k}u_k \lesssim \sum_{k=1}^{N}\Big(\|u_k-P_1u_k\|_1+\|u_k-u_k^{(0)}\|_0+|\lambda_k-\lambda_k^{(0)}|\Big),$$

which means (A.6) since $u=\sum_{k=1}^{N}\alpha_{i,k}u_k\in V$. This completes the proof. □

REFERENCES

[1] R.A. Adams, *Sobolev Spaces*, Academic Press, New York, 1975.

[2] S. Agmon, *Lectures on the Exponential Decay of Solutions of Second-Order Elliptic Operators*, Princeton University Press, Princeton, 1981.

[3] C.O. Almbladh and U. von Barth, *Exact results for the charge and spin densities, exchange-correlation potentials, and density-functional eigenvalues*, Phys. Rev. B, **31** (1985), pp. 3231-3244.

[4] O.K. Andersen, *Linear methods in band theory*, Phys. Rev. B, **12** (1975), pp. 3060-3083.

[5] P.E. Blöchl, *Projector augmented-wave method*, Phys. Rev. B, **50** (1994), pp. 17953-17979.

[6] D.R. Bowler and T. Miyazaki, *$O(N)$ methods in electronic structure calculations*, Report Prog. Pgys., **75** (2012), pp. 036503-03645.

[7] J.M. Cascon, C. Kreuzer, R.H. Nochetto, and K.G. Siebert, *Quasi-optimal convergence rate for an adaptive finite element method*, SIAM J. Numer. Anal., **46** (2008), pp. 2524-2550.

[8] H. Chen, X. Dai, X. Gong, L. He, and A. Zhou, *Adaptive finite element approximations for Kohn-Sham models*, arXiv:1302.6896, Multi. Model. Simul., to appear.

[9] H. Chen, L. He, and A. Zhou. *Finite element approximations of nonlinear eigenvalue problems in quantum physics*, Comput. Meth. Appl. Mech. Engrg., **200** (2011), pp.1846-1865.

[10] X. Dai, X. Gong, Z. Yang, D. Zhang and A. Zhou, *Finite volume discretizations for eigenvalue problems with applications to electronic structure calculations*, Mult. Model. Simul., **9**(2011), pp.208-240.

[11] X. Dai, L. Shen, and A. Zhou, , *A local computational scheme for higher order finite element eigenvalue approximations*, Int. J. Numer. Anal. Model., **5**(2008), pp. 570-589.

[12] X. Dai, J. Xu, and A. Zhou, *Convergence and optimal complexity of adaptive finite element eigenvalue computations*, Numer. Math., **110** (2008), pp. 313-355.

[13] X. Dai and A. Zhou, *Three-scale finite element discretizations for quantum eigenvalue problems*, SIAM J. Numer. Anal., **46** (2008), pp. 295-324.

[14] W. Dörfler, *A convergent adaptive algorithm for Poisson's equation*. SIAM J. Numer. Anal., **33** (1996), pp. 1106-1124.

[15] E.M. Garau, P. Morin, and C. Zuppa, *Convergence of adaptive finite element methods for eigenvalue problems*, M^3AS, **19** (2009), pp. 721-747.

[16] Gaussian, http://gaussian.com/.

[17] P. Hohenberg and W. Kohn, *Inhomogeneous electron gas*, Phys. Rev. B., **136**(1964), pp. 864-871.

[18] E. Kaxiras, *Atomic and Electronic Structure of Solids*, Cambridge University Press, Cambridge, UK, 2003.

[19] W. Kohn and L. J. Sham, *Self-consistent equations including exchange and correlation effects*, Phys. Rev. A., **140**(1965), pp. 4743-4754.

[20] G. Kresse and J. Furthmüller, *Efficient iterative schemes for ab initio total-energy calculations using a plane-wave basis set*, Phys. Rev. B., **54**(1996), pp. 11169-11186.

[21] C. Le Bris (ed.), *Handbook of Numerical Analysis, Vol. X. Special issue: Computational Chemistry*, North-Holland, Amsterdam, 2003.

[22] S.A. Losilla and D. Sundholm, *A divide and conquer real-space approach for all-electron molecular electrostatic potentials and interaction energies*, J. Chem. Phys., **136** (2012), pp. 214104-214103.

[23] R. Martin, *Electronic Structure: Basic Theory and Practical Methods*, Cambridge university Press, London, 2004.

[24] M. C. Payne, M. P. Teter, D. C. Allan, T. A. Arias, and J. D. Joannopoulos, *Iterative minimization techniques for ab initio total-energy calculations: molecular dynamics and conjugate gradients*, Rev. Mod. Phys., **64** (1992), pp.1045-1097.

[25] R. G. Parr and W. T. Yang, *Density-Functional Theory of Atoms and Molecules*, Clarendon Press, Oxford, 1994.

[26] J. P. Perdew and A. Zunger, *Self-interaction correction to density-functional approximations for many-electron systems*, Phys. Rev. B, **23**(1981), pp. 5048-5079.

[27] PHG,*http://lsec.cc.ac.cn/phg/*.

[28] N. Troullier and J.L. Martins, *Efficient pseudopotentials for plane-wave calculations*, Phys. Rev. B, **43** (1991), pp. 1993-2006.

[29] D. Vanderilt, *Soft slef-consistent pseudopotentials in a generalized eigenvalue formalism*, Phys. Rev. B, **41** (1990), pp. 7892-7895.

[30] H. Yserentant, *Regularity and Approximability of Electronic Wave Functions*, Lecture Notes in Mathematics, **2000**, Springer-Verlag, Berlin, 2010.